BIOLOGY, MEDICINE, & NATURAL PRODUCT CHEMISTRY ISSN 2089-6514 (paper)
Volume 14, Number 2, October 2025 | Pages: 1427-1435 | DOI: 10.14421/biomedich.2025.142.1427-1435 ISSN 2540-9328 (online)

In Silico Study of the Antibacterial Activity of Bioactive Compounds from *Portulaca oleracea* L. Herb Extract against Propionibacterium Acnes

Nadhifa Dini Maulida, Nur Aqidah, Nanda Ma'rifatul Ilmiah, Maprilia Nur Nabillah, Niken Ayu Ramadhany, Mohammad Rofik Usman*
Department of Pharmacy, Faculty of Health Sciences, Universitas dr. Soebandi,
Jl. dr. Soebandi No 99 Jember 6811, Tel. 0331-483536, Indonesia.

Corresponding author*
mrofik05@gmail.com

Manuscript received: 18 November, 2025. Revision accepted: 10 December, 2025. Published: 24 December, 2025.

Abstract

Acne vulgaris is a common dermatological condition primarily caused by the bacterium *Propionibacterium acnes*. The use of natural compounds as alternative therapies has gained attention due to their lower side effects compared to synthetic agents. This study aimed to evaluate the antibacterial potential of bioactive compounds present in purslane (*Portulaca oleracea* L.) herbs against *P. acnes* through an in silico approach. Out of 15 identified compounds, 12 satisfied Lipinski's parameters, and 9 compounds were selected for further analysis. Pharmacokinetic and toxicity predictions were performed using the pkCSM platform to determine the ADMET profiles, while ligand–receptor interactions were analyzed via molecular docking against the *Exo-x-sialidase* protein target (PDB ID: 7LBV). The ADMET prediction results indicated that most compounds exhibited good solubility, high absorption, moderate skin permeability, and favorable distribution and metabolism profiles. Docking visualization revealed the presence of hydrogen bonds and hydrophobic interactions with key residues at the receptor's active site. Interestingly, *butylated hydroxytoluene* demonstrated the lowest binding energy (–6.56 kcal/mol), which was better than that of the positive control (–6.17 kcal/mol), indicating a stronger binding affinity. Overall, Portulaca oleracea shows promise as a natural source of antibacterial compounds against *P. acnes*, warranting further in vivo investigation.

Keywords: *Portulaca oleracea*; Propionibacterium acnes; ADMET; in silico; molecular docking.

INTRODUCTION

Acne is an inflammatory infection of the sebaceous glands, characterized by obstruction and the accumulation of keratinous material caused by the bacterium Propionibacterium acnes (*P. acnes*) (Goodarzi et al., 2020). In Indonesia, approximately 80–85% of adolescents experience acne, with the highest prevalence occurring among individuals aged 15–18 years, women over 25 years, and around 3% among those aged 35–44 years (Kurniawati et al., 2022). Adolescents affected by acne often face various psychological and social impacts, including reduced quality of life and lower self-esteem. Quality of life refers to an individual's perception of their position in life within the context of their culture, values, goals, expectations, and personal standards, while self-esteem represents how individuals evaluate their self-worth, particularly in terms of physical appearance (Autrilia & Ninin, 2022).

Although several methods exist to prevent acne, there is currently no complete or permanent cure for this condition. Some approaches involve the topical application of anti-acne creams containing salicylic acid as the active ingredient (Li et al., 2022). However, salicylic acid-based formulations are associated with several side effects, including dryness, irritation, and skin peeling (Nareswari et al., 2023). Therefore, natural ingredients are increasingly being explored as alternative therapeutic agents due to their lower risk of adverse effects compared to synthetic compounds (Syal et al., 2020).

Given the high prevalence of acne cases, preventive and therapeutic strategies are essential to reduce the incidence rate, particularly among adolescents in Indonesia. One preventive approach involves inhibiting the bacterial autolysis process, in which bacterial cell rupture caused by lipase enzyme activity contributes to the formation of new acne lesions (Mavranezouli et al., 2022). To inhibit autolysis in *P. acnes*, the Exo-x-sialidase receptor (PDB ID: 7LBV) plays a key role and has been identified as a potential target for antibacterial compounds (Yu et al., 2022).

Several plants have been reported to possess antibacterial properties and can serve as active

ingredients in the formulation of antibacterial facial wash products targeting *P. acnes*, such as *Talinum triangulare* (purslane) (Enengedi et al., 2022). Additionally, *Portulaca oleracea* L. (common purslane) from the Portulacaceae family has shown antibacterial potential, although its utilization remains limited (Ojah et al., 2021). Therefore, *Portulaca olerecea* was selected as a promising natural source of bioactive compounds for potential development into antibacterial agents.

In this study, the identification of bioactive compounds from P. oleracea with potential antibacterial activity against *P. acnes* was carried out through in silico screening and analysis. The in silico approach enables rapid and accurate prediction of ligand–receptor interactions (Krihariyani et al., 2020). Furthermore, a positive control was included to validate the docking results and ensure the accuracy of the simulation. Clindamycin was used as the positive control against *P. acnes* (Abbas et al., 2020).

MATERIALS AND METHODS

Materials

The receptor structure used in this study was Exo-x-sialidase (PDB ID: 7LBV), with the native ligand 2-Deoxy-2,3-Dehydro-N-Acetyl-Neuraminic Acid (DAN). Clindamycin was employed as the positive control. A total of 15 compounds were obtained from GC–MS analysis of *Portulaca oleracea* L. extract and compared with compounds reported by Osman et al. (2023).

Tools

The hardware used in this study consisted of a personal computer, while the software included autodock 4.2.6, molegro molecular viewer, discovery studio 2024, marvinsketch, PyRx, and notepad++. The pubChem database was utilized to obtain the chemical structures of the tested compounds, and the RCSB Protein Data Bank was used to retrieve the receptor structure. The pkCSM web server was employed to predict pharmacokinetic and ADMET profiles.

Procedures

Drug-likeness Screening and Pharmacokinetic Profile Prediction

The parameters of the 15 candidate compounds were evaluated based on Lipinski's Rule of Five using the Lipinski web server. The criteria included Log P (<5), molecular weight (<500 Da), hydrogen bond donors (<5), molar refractivity between 40–130, and hydrogen bond acceptors (<10). Compounds meeting these criteria were considered to possess acceptable physicochemical properties and potential drug-likeness for further evaluation.

Pharmacokinetic prediction was conducted using the pkCSM web server to obtain a comprehensive overview of the pharmacokinetic and toxicity profiles of each compound. The results included absorption, distribution, metabolism, excretion, and toxicity (ADMET) parameters, providing insights into the compounds' potential safety and suitability for further development as antibacterial agents.

Receptor and Natural Ligand Preparation

The Exo-x-sialidase receptor was downloaded from the RCSB Protein Data Bank (PDB ID: 7LBV). The protein structure was separated from its native ligand using Molegro Molecular Viewer, and the resulting file was saved in .pdb format. Following the separation process, hydrogen atoms were added to both the native ligand and the receptor using Discovery Studio to optimize the structure for subsequent docking analysis.

Ligand Preparation

The compounds were downloaded in two-dimensional (2D) format from the PubChem database. The downloaded files were opened using MarvinSketch software, then protonated to achieve a physiological pH of 7.4. Each ligand structure was saved in .mrv format within a designated ligand folder. Subsequently, conformational analysis was performed to identify the lowest-energy conformation, and the optimized structures were saved in .mol2 format for further molecular docking analysis.

Docking Validation

Docking validation was performed using AutoDockTools by re-docking the native ligand into the active site of the protein, employing a grid box size adjusted to the dimensions of the test ligands. The final outcome of the docking validation was expressed as the Root Mean Square Deviation (RMSD) value in angstroms (Å). The molecular docking method is considered valid when the RMSD value is ≤ 2 Å (Ruswanto et al., 2022).

In this study, the lowest RMSD value obtained was 0.57 Å at run number 53, indicating high docking accuracy. The best docking result of the native ligand was saved in .pdb format and subsequently used to define the grid box for docking of the test ligands. The docking result of the native ligand was then visualized using Discovery Studio and compared with the pre-docked native ligand structure to confirm the alignment and binding position consistency.

Virtual Screening

Virtual screening of the test ligands was carried out by performing molecular docking with 100 runs for each ligand against the same target protein used for the native ligand. The docking simulations were conducted using the PyRx software, employing the Lamarckian Genetic Algorithm (GA) without repetition. The output of this stage included the binding free energy (BFE) or ΔG values, expressed in kcal/mol, as well as the inhibition constant (KI) values for each ligand.

Docking Visualization and Interaction Analysis

Visualization and interaction analysis of the docking results were conducted to observe the binding process between the reference ligand and the test ligands. The visualization results revealed interactions between the amino acid residues and the ligands. The contacts formed between these residues and the ligands indicated a potential inhibitory activity on the Exo-x-sialidase receptor. Hydrogen bonds and hydrophobic interactions play a crucial role in stabilizing ligand–receptor binding and supporting biomolecular responses, such as protein activation.

Protein Analysis

Protein analysis was performed using the PDBsum web server to obtain statistical data regarding the structural quality of the receptor protein. A well-validated protein model is characterized by having more than 90% of its residues located in the most favored regions and less than 0.8% in the disallowed regions of the Ramachandran plot (Komalasari et al., 2024).

RESULTS AND DISCUSSION

Drug screening and pharmacokinetic profile prediction

Drug-likeness screening and pharmacokinetic prediction were performed to evaluate the parameters required for each compound to be considered a potential candidate for further analysis. According to the study by Osman et al. (2023), GC–MS analysis of *Portulaca oleracea* herb extract identified a total of 69 compounds. However, only 31 compounds met the specified parameter values, with the most common deviation observed in the Log P parameter.

Among the 31 compounds that satisfied the criteria, only 9 were selected for molecular docking analysis because the remaining 21 compounds contained silicon (Si) atoms. This exclusion was based on the fact that most molecular docking programs are optimized for organic compounds (Chairunisa et al., 2023). Consequently, pharmacokinetic prediction using the ADMET model (Absorption, Distribution, Metabolism, Excretion, and Toxicity) was conducted exclusively on the 9 selected test compounds, along with one positive control compound. The Lipinski parameter data of the nine selected compounds are presented in table 1.

Table 1. Lipinski's parameter data.

Compound	Log P (<5)	Molecular weight/mass (g/mol) (<500)	Hydrogen Bond Donor (<5)	Molar Refractory Between (40-130)	Hydrogen Bond Acceptor (<10)
Diacetone alcohol (Compound 1)	0,7364	116,16	1	49,52	2
Benzaldehyde, 3-benzyloxy-2-fluoro-4-methoxy-(Compound 2)	3,2258	260,264	0	110,137	3
Benzyl iodide (Compound 3)	2,6216	218,037	0	63,058	0
Lauryldimethylamine (Compound 4)	4,4689	213,409	0	97,243	1
Bisabolol oxide A (Compound 5)	4,2684	238,371	0	105,744	2
D-Carvone (Compound 6)	2,4879	150,221	0	67,8	1
Isospathulenol (Compound 7)	3,5299	220,356	1	98,936	1
Butylated Hydroxytoluene (Compound 8)	4,29562	220,356	1	99,51	1
Diisobutyl phthalate (Compound 9)	3,3122	278,348	0	119,631	4
Clindamycin (positive control)	0,3895	424,991	4	7	7

Table 2. Prediction ADMET.

Compound	Water solubility	Skin Permeability	AMES toxicity	Skin Sensitisation
Compound 1	0,14	-3,323	No	Yes
Compound 2	-3,828	-2,306	No	No
Compound 3	-3,2	-1,866	No	Yes
Compound 4	-5,469	-1,757	No	Yes
Compound 5	-4,491	-1,762	No	Yes
Compound 6	-2,324	-2,145	No	Yes
Compound 7	-0,928	-2,107	Yes	No
Compound 8	-2,736	-2,735	Yes	No
Compound 9	-4,407	-2,645	No	No
Positive control	-2.959	-2,888	No	No

Based on the ADMET prediction results presented in table 2, several parameters were evaluated, including water solubility, skin permeability, AMES toxicity, and skin sensitization. In terms of water solubility, compounds

with higher values are more easily formulated in aqueous-based preparations. Compound 1 (0.14) and compound 7 (–0.928) exhibited better solubility compared to other compounds, whereas compound 4 (–5.469) and compound 5 (–4.491) showed poor solubility, making them less suitable for water-based formulations.

The skin permeability values of all compounds were within the safe range (–1.757 to –3.323), with the positive control showing –2.888. Compounds 1, 8, and 9 demonstrated lower permeability, which is ideal for topical applications, as it prevents excessive skin penetration. Regarding genotoxic safety, the AMES toxicity results indicated that all compounds were non-mutagenic except for compounds 7 and 8, which showed potential mutagenic effects.

The skin sensitization parameter showed that compounds 1, 3, 4, 5, and 6 have the potential to cause skin irritation, while compounds 2, 7, 8, and 9 were found to be non-sensitizing. Overall, when compared to the positive control, compounds 2 and 9 exhibited the most favorable ADMET profiles for facial wash formulations. Both compounds possessed good water solubility, low skin permeability, and no indications of mutagenicity or skin irritation, making them the most promising candidates for topical formulation.

In silico analysis

The receptor used in the in silico analysis is shown in figure 1, and the corresponding native ligand is presented in figure 2. The ligands of the test compounds underwent protonation to match the physiological blood pH of approximately 7.4, followed by conformational optimization to determine the lowest-energy conformation. This optimization was conducted to obtain the most stable three-dimensional structure of each ligand with the lowest potential energy. A lower conformer energy indicates a more stable ligand structure, thereby providing a more representative interaction with the receptor's active site. The resulting data are presented in table 3.

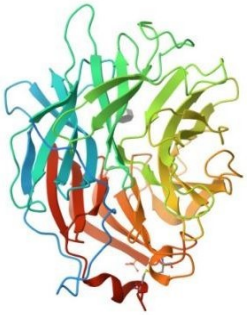

Figure 1. Receptor 7LBV.

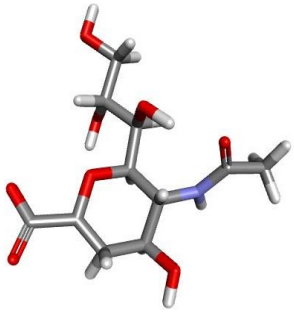

Figure 2. Native ligand.

Table 3. Ligand Preparation Results.

Compound Identification	Energy conformers (kcal/mol)	Interpretation of Stability	3D Structure
Compound 4	5,61	Highly stable	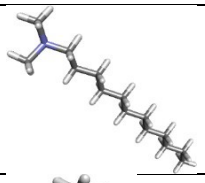
Compound 1	10,07	Stable	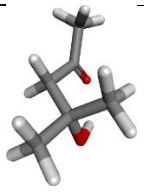
Compound 5	15,07	Moderately stable	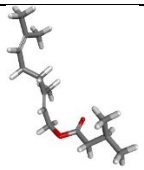
Compound 6	26,76	Less stable	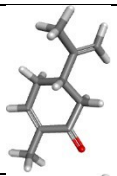
Compound 3	28,01	Less stable	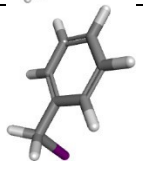

Compound Identification	Energy conformers (kcal/mol)	Interpretation of Stability	3D Structure
Compound 9	34,28	Unstable	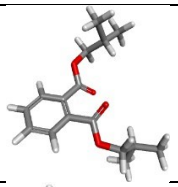
Compound 8	54,52	Unstable	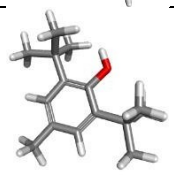
Compound 2	76,46	Unstable	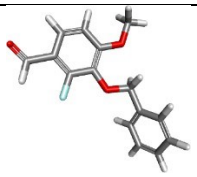
Compound 7	84,01	Unstable	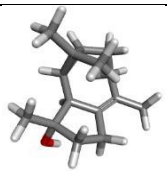
Kontrol positif	145,43	Unstable	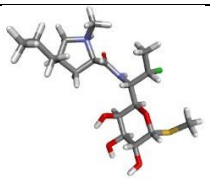

The ligand conformational optimization stage was conducted to determine the most stable three-dimensional (3D) structure of each compound derived from *Portulaca oleracea* L. The lower the conformer energy value (kcal/mol), the more stable the ligand structure. In the results obtained, the conformer energy values ranged from 5.61 to 145.43 kcal/mol. A conformer is considered stable when the energy difference between conformations is ≤ 5 kcal/mol from the minimum energy position (Rehman et al., 2023). Higher conformational energy values indicate a relatively lessstable molecular structure.

The optimization results showed that the conformer energies of the test compounds ranged between 5.61 and 145.43 kcal/mol. A lower conformer energy corresponds to a more stable molecular structure, as less potential energy is required to maintain its three-dimensional conformation. According to the literature, a conformer is considered stable when its energy difference does not exceed 5–10 kcal/mol from the lowest-energy conformer. In this study, Compound 4 (5.61 kcal/mol) exhibited the highest stability, followed by Compound 1 (10.07 kcal/mol), which was still categorized as stable. Other compounds, such as compounds 5 and 6, showed moderate stability with conformer energies between 15–26 kcal/mol, whereas compounds 7, 8, and 9 exhibited high energy values (>50 kcal/mol), indicating lower structural stability. Higher conformational energy values suggest greater molecular rigidity and bond strain, making the structure less energetically efficient. Nevertheless, compounds with higher conformational energy may still exhibit strong biological activity if they form highly stable interactions with the receptor.

Docking validation

The docking validation of the native ligand produced a grid box size of 40 × 40 × 40 Å with grid center coordinates at x = –21.339, y = 9.69 and z = 17.549 Å. The validation results yielded a Root Mean Square Deviation (RMSD) value of 0.57 Å with the lowest binding energy of –9.52 kcal/mol, obtained at run number 53. This RMSD value indicates valid docking accuracy, as it falls below the 2 Å threshold (Ruswanto et al., 2022).

The re-docking process confirmed structural alignment consistency between the pre-docked and re-docked conformations, showing only minimal changes in the binding pose. Therefore, the docking validation was considered reliable, and the grid box parameters were

subsequently used for further docking simulations of the test ligands.

Figure 3. Overlay of the re-docking results showing the DAN conformation before (red) and after (yellow).

Virtual screening

The docking process for the test ligand and positive control was performed with 100 runs. The parameters to be observed were the binding free energy (ΔG) and KI (μM). The docking results are presented in table 4.

Table 4. Docking results data.

Compound	Running	ΔG (kkal/mol)	KI (μM)
Compound 1	68	-3,78	1690
Compound 2	48	-5,76	60,36
Compound 3	10	-4,12	959,33
Compound 4	73	-4,28	729,32
Compound 5	2	-5,34	121,70
Compound 6	53	-5,22	149,47
Compound 7	56	-5,83	53
Compound 8	82	-6,56	15,46
Compound 9	87	-5,21	151,62
Positive control	50	-6,17	29,88

The stability of the interaction between the ligand and the target receptor was predicted through binding free energy analysis, as indicated by low ΔG values. Among the nine test compounds, compound 8 exhibited superior binding energy (ΔG) compared to the positive control, with a binding energy of -6.56 kcal/mol and a KI of 15.46 μM. This suggests that the compound has greater potential than the positive control and may serve as an inhibitor of the target protein *P. acnes*.

Visualization of docking results

Visualization results revealed that compound 8 was the most prominent, demonstrating strong anchoring at the active site, primarily through hydrophobic interactions with nonpolar residues surrounding the protein pocket. This supports its role as a potential inhibitor of the target enzyme *P. acnes*. Additionally, compound 8 displayed similar interactions in the alkyl bond with the amino acid A:ALA147. Apart from compound 8, compound 5 showed the most interaction similarity with the positive control, including conventional hydrogen bonds with amino acids A:TYR423 and A:ARG329, Alkyl interactions with A:ALA147, and carbon–hydrogen bonds with A:ASP146. However, compound 5 exhibited binding energy values that were not superior to the positive control. Therefore, compound 8 can be considered the most promising compound compared to the positive control.

Table 5. Visualization of Amino Acid Interactions.

Compound Name		Ligand interaction	2D
Compound 1	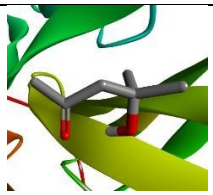	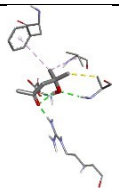	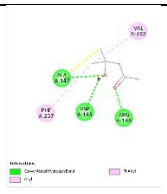
Compound 2	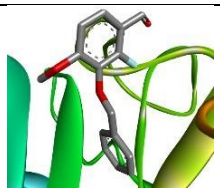	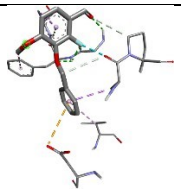	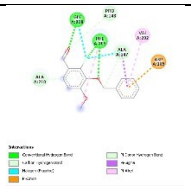
Compound 3	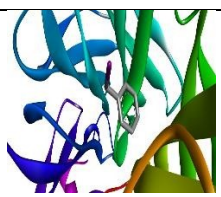	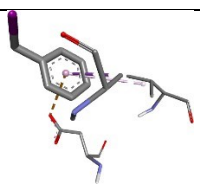	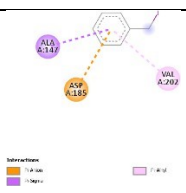

Compound Name		Ligand interaction	2D
Compound 4	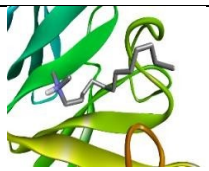	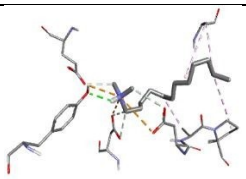	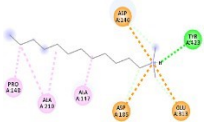
Compound 5	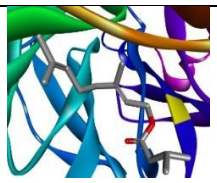	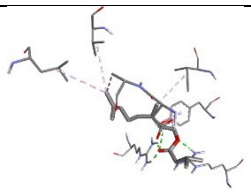	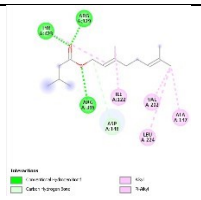
Compound 6	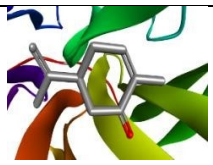	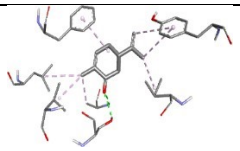	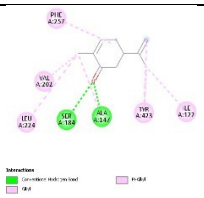
Compound 7		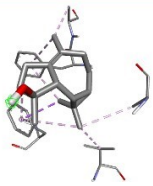	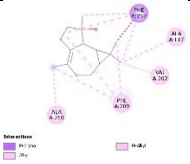
Compound 8	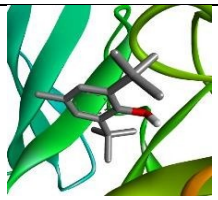	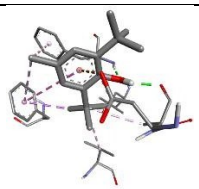	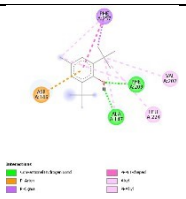
Compound 9	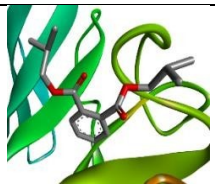		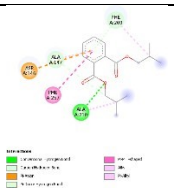
Positive control	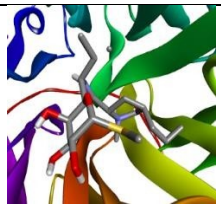	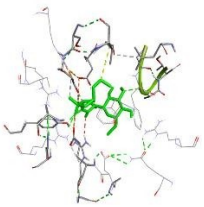	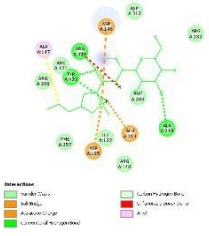

Table 6. Hydrogen Bonding and Hydrophobic Interactions of Compounds.

Compound	Conventional Hydrogen Bond	Alkyl	Carbon Hydrogen Bond	Attractive Charge
Compound 1	**A:ARG140** (1,723572); A:ASP185 (2,100523); A:ALA147 (2,217005)	**A:ALA147** (3,330106); A:VAL202 (4,783842)		
Compound 2	A:PHE209 (2,447017); A:PHE209 (2,124201); **A:GLY208** (2,375328)		A:ALA147 (3,720319); A:PRO148 (3,724696)	
Compound 3				

Compound	Conventional Hydrogen Bond	Alkyl	Carbon Hydrogen Bond	Attractive Charge
Compound 4	**A:TYR423** (2,340302)	A:PRO148 (5,395796); A:ALA210 (4,272301); A:ALA210 (4,906233); **A:ALA147** (3,984995)	**A:ASP185** (3,143153); A:GLU313 (2,748170); **A:ASP146** (3,405493)	**A:ASP185** (3,741780); A:GLU313 (3,674814); **A:ASP146** (4,366836)
Compound 5	A:ARG395 (2,188913); **A:TYR423** (2,521789); **A:ARG329** (2,234332); **A:ARG329** (1,899263)	**A:ALA147** (3,504774); A:LEU224 (4,765008); A:VAL202 (4,482326); A:ILE122 (4,558296)	**A:ASP146** (3,585321)	
Compound 6	**A:SER184** (2,415664); A:ALA147 (1,911880)	A:ILE122 (4,334648); A:LEU224 (4,460332); A:VAL202 (3,463026); **A:ALA147** (3,395563)		
Compound 7		**A:ALA147** (4,439083); A:VAL202 (4,313931); A:ALA210 (4,276128)		
Compound 8	A:ALA147 (1,847992); A:PHE209 (2,023923)	**A:ALA147** (4,119307); A:VAL202 (4,749704); A:LEU224 (5,275508)		
Compound 9	**A:ALA210** (2,193544)	A:ALA210 (3,846283)	A:ALA147 (3,336596)	

Protein analysis

Based on the Ramachandran plot, the percentage of residues in the favored, allowed, and disallowed regions for 7LBV can also be observed in Figure 4. From Figure 4, it can be seen that 7LBV has 87.4% of residues in the favored regions and 0.0% in the disallowed regions. In conclusion, the quality of 7LBV can be evaluated based on the theory stating that a good-quality protein should have more than 90% of residues in the most favored regions and less than 0.8% in disallowed regions (Zaheer et al., 2023). Therefore, the percentage of residues in the most favored regions does not meet the ideal criterion. However, the quality of 7LBV can still be considered acceptable because there are no residues in the disallowed regions.

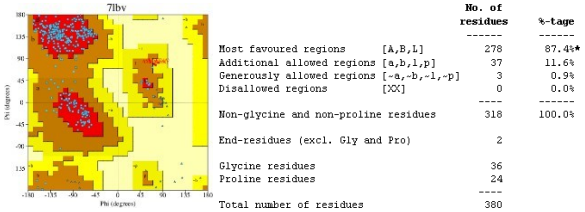

Figure 4. Amachandran plot statisticrlay of the re-docking results showing the DAN conformation before (red).

CONCLUSIONS

GC-MS analysis of *Portulaca oleracea* L. (purslane) revealed 15 compounds, of which 12 met Lipinski's parameters, and 9 compounds were suitable for further testing. ADMET predictions showed that most compounds exhibited good solubility, skin permeability, AMES toxicity, and skin sensitization profiles, with compounds 2 and 9 demonstrating the most favorable properties. Furthermore, docking results indicated that *butylated hydroxytoluene* (compound 8) had the lowest binding energy (-6.56 kcal/mol), which was better than the positive control, *clindamycin* (-6.17 kcal/mol), indicating a stronger binding affinity toward the Exo-x-sialidase receptor (PDB 7LBV). Additionally, the similarity of interactions between compound 8 and the positive control, particularly in the alkyl bond with amino acid A:ALA147, further confirms that compound 8 is the most promising candidate. Therefore, *Portulaca oleracea* shows significant potential as a source of natural antibacterial compounds that are effective and safe for development in acne therapy. However, these findings still require validation through in vitro and in vivo studies to confirm the biological activity and safety of the compounds comprehensively.

Acknowledgements: The authors would like to express their gratitude to the Faculty of Health Sciences, Universitas dr. Soebandi Jember, for providing research facilities, as well as to all parties who have assisted in the preparation of this article.

Authors' Contributions: All authors contributed significantly to the preparation of this manuscript. The first author was responsible for theresearch design, in silico analysis, and drafting of the main manuscript. The second author handled the ADMET data processing and

validation of the docking results. The third author contributed to the literature analysis, backgrounddevelopment, and research methodology. The fourth author carried out the visualization of the docking results and contributed to the preparation of the results and discussion sections. The fifth author performed manuscript editing, conclusion writing, and language refinement. In addition, the supervising lecturer provided guidance, scientific advice, and substantive corrections to ensure the research was conducted according to its objectives. All authors and the supervising lecturer have read and approved the final version of this article and declare that there is no conflict of interest.

Funding: This article was created with grant funds obtained from Belmawa as PKM funding.

Competing Interests: The authors declare that there are no competing interests.

REFERENCES

Abbas, R. A., Khalaf, W. S., Ibrahim, S. M., Radwan, S. R., & Afifi, S. S. 2020. The Effect of Antibiotic/Antiseptic Combination on *Propionibacterium Acnes* to Overcome Antibiotic Resistance. *J App Pharm*, 12, 57–68.

Autrilia, R., & Ninin, R. 2022. Eksplorasi Dampak Psikologis pada Remaja yang memiliki Masalah Penampilan dengan Jerawat. *Jurnal Psikologi Udayana*, 9(2), 194–205.

Chairunisa, F., Safithri, M., Andrianto, D., Kurniasih, R., & Irsal, R. A. P. 2023. Molecular Docking of Red Betel Leaf Bioactive Compounds (Piper Crocatum) as Lipoxygenase Inhibitor. Indonesian *Journal Of Pharmaceutical Science And Technology*, 10(2), 90–103.

Enengedi, I. S., Ekpa, O. D., & Akpabio, U. D. 2022. Formulation and Evaluation of in Vivo Hydration Property of Creams with *Talinum triangulare* and *Dacryodes edulis* Extracts. *Journal Of Medicinal Plants Studies*, 10 (2), 151–158.

Goodarzi, A., Mozafarpoor, S., Bodaghabadi, M., & Mohamadi, M. 2020. The Potential of Probiotics for Treating Acne Vulgaris: A Review of Literature on Acne and Microbiota. *Dermatologic Therapy*, 33(3), E13279.

Komalasari, E., Susanti, & Mardianingrum, R. 2024. Uji In Silico Turunan Kuersetin sebagai Penurun Kolesterol LDL dari Kulit Jeruk Manis (*Citrus Sinensis*). *Jurnal Penelitian Farmasi Indonesia*, 13(1), 46–56.

Krihariyani, D., Wasito, E. B., Siswodihardjo, S., Yuniarti, W. M., & Kurniawan, E. 2020. In Silico Study on Antibacterial Activity and Brazilein ADME of Sappan Wood (*Caesalpinia sappan* L.) Against *Escherichia Coli* (Strain K12). *Systematic Reviews In Pharmacy*, 11(10), 290–296.

Kurniawati, S. L., An, D., Sukmawati, N., Marita, I., Luba, R., No, S., Kediri, K., & Timur, J. 2022. Uji Aktivitas Ekstrak Etanol Akar Bajakah Tampala (*Spatholobus Littoralis* Hassk) sebagai Antibakteri *Propionibacterium Acnes* dengan Metode Difusi. *Java Health Journal*. Vol 3.

Li, W., Yu, Q., Shen, Z., Zhang, L., Zhang, W., & Li, C. 2022. Efficacy and Safety of a Cream Containing Octyl Salicylic Acid, Salicylic Acid, Linoleic Acid, Nicotinamide, and Piroctone Olamine Combined With 5% Benzoyl Peroxide in the Treatment of Acne Vulgaris: A Randomized Controlled Study. *Chinese Medical Journal*, 135(11), 1381–1382.

Mavranezouli, I., Daly, C. H., Welton, N. J., Deshpande, S., Berg, L., Bromham, N., Arnold, S., Phillippo, D. M., Wilcock, J., & Xu, J. 2022. A Systematic Review and Network Meta-Analysis of Topical Pharmacological, Oral Pharmacological, Physical and Combined Treatments for Acne Vulgaris. *British Journal Of Dermatology*, 187(5), 639–649.

Nareswari, T. L., Vrince, F. O., & Syafitri, E. 2023. Formulation and Evaluation of Citronella Oil (*Cymbopogon Nardus* (L.) Rendle) Cream for Acne Treatment. *International Journal Of Drug Delivery Technology*, 13(1), 419–422.

Ojah, E. O., Oladele, E. O., & Chukwuemeka, P. 2021. Phytochemical and Antibacterial Properties of Root Extracts from *Portulaca Oleracea* Linn. (Purslane) Utilised in the Management of Diseases in Nigeria. *Journal Of Medicinal Plants For Economic Development*, 5(1), 103.

Osman, A., Abdelkader, A., Abdel-Raouf, Mohamed, & Elbana, Magdy. 2023. Phytochemical Screening and Antibacterial Activity of *Portulaca Oleracea* L. Extracts Against Antibiotic-Resistant Bacteria. *Alfarama Journal Of Basic & Applied Sciences*, 0(0), 0–0.

Rehman, H. M., Rehman, H. M., Ahmed, N., & IMRAN, M. 2023. In Silico Design and Evaluation of Novel Cell Targeting Melittin-Interleukin-24 Fusion Protein: A Potential Drug Candidate Against Breast Cancer. *Sains Malaysiana*, 52(11), 3223–3237.

Ruswanto, R., Mardianingrum, R., & Yanuar, A. 2022. Computational Studies of Thiourea Derivatives as Anticancer Candidates Through Inhibition of Sirtuin-1 (SIRT1). *Jurnal Kimia Sains dan Aplikasi*, 25(3), 87–96.

Syal, S., Pandit, V., & Ashawat, M. S. 2020. Traditional Herbs to Treat Acne Vulgaris. *Asian Journal Of Pharmaceutical Research*, 10(3), 195–201.

Yu, A. C. Y., Volkers, G., Jongkees, S. A. K., Worrall, L. J., Withers, S. G., & Strynadka, N. C. J. 2022. Crystal Structure of The *Propionibacterium Acnes* Surface Sialidase, a Drug Target for *P. Acnes-Associated Diseases*. *Glycobiology*, 32(2), 162–170.

Zaheer, M., Ali, N., Javed, H., Munir, R., & Jamil, N. 2023. Uncovering the Impact of SARS-Cov2 Spike Protein Variants on Human Receptors: A Molecular Dynamics Docking and Simulation Approach. *Journal of Infection and Public Health*, 16(10), 1544–1555.

THIS PAGE INTENTIONALLY LEFT BLANK